



**HAL**  
open science

## Neutron scattering and cation rotational motion in tetramethylammonium manganese chloride

B. Lassier, C. Brot, J.W. White

► **To cite this version:**

B. Lassier, C. Brot, J.W. White. Neutron scattering and cation rotational motion in tetramethylammonium manganese chloride. *Journal de Physique*, 1973, 34 (5-6), pp.473-481. 10.1051/jphys:01973003405-6047300 . jpa-00207409

**HAL Id: jpa-00207409**

**<https://hal.science/jpa-00207409v1>**

Submitted on 4 Feb 2008

**HAL** is a multi-disciplinary open access archive for the deposit and dissemination of scientific research documents, whether they are published or not. The documents may come from teaching and research institutions in France or abroad, or from public or private research centers.

L'archive ouverte pluridisciplinaire **HAL**, est destinée au dépôt et à la diffusion de documents scientifiques de niveau recherche, publiés ou non, émanant des établissements d'enseignement et de recherche français ou étrangers, des laboratoires publics ou privés.

Classification  
*Physics Abstracts*  
 48.2

## NEUTRON SCATTERING AND CATION ROTATIONAL MOTION IN TETRAMETHYLAMMONIUM MANGANESE CHLORIDE

B. LASSIER (\*) and C. BROT (\*)

Laboratoire de Physicochimie des Rayonnements  
 Université Paris-Sud, 91405 Orsay, France

and

J. W. WHITE

Physical Chemistry Laboratory, Oxford (England)

(Reçu le 28 septembre 1972, révisé le 15 décembre 1972)

**Résumé.** — La diffusion des neutrons par un échantillon polycristallin de chlorure de manganèse tétraméthylammonium a été mesurée pour des transferts d'énergie compris entre 0 et  $500\text{ cm}^{-1}$ , en dessous et au-dessus de la transition de phase à 128 K. Dans la région  $0\text{--}50\text{ cm}^{-1}$ , qui reflète le mouvement rotationnel des cations polyatomiques, le spectre diffusé présente un pic inélastique en basse température, mais seulement un épaulement prolongeant la zone quasi élastique en phase haute température.

Ces spectres sont interprétés semi-quantitativement par un modèle qui suppose que les ions tétraméthylammonium sont soumis à un champ cristallin à trois puits et à des impulsions aléatoires de couple pour simuler le contact avec le bain thermique. L'ajustement du modèle aux résultats expérimentaux indique que la barrière de potentiel est assez haute en phase basse température pour que les cations restent longtemps en état de libration dans un des puits. En phase haute température par contre le mouvement est celui d'un rotateur faiblement gêné.

**Abstract.** — The scattering of neutrons by a polycrystalline sample of tetramethylammonium manganese chloride has been measured for  $0\text{--}500\text{ cm}^{-1}$  energy transfers, both below and above the phase transition at 128 K. In the  $0\text{--}50\text{ cm}^{-1}$  region, which reflects the rotational motion of the polyatomic cations, the scattered spectrum exhibits an inelastic peak at low temperature, but only a shoulder extending from the quasi-elastic peak in the high temperature phase.

These spectra are semi-quantitatively interpreted by a model which assumes that the tetramethylammonium ions experience a three-well crystalline field and random torque-impulses for simulating the contact with the thermal bath. The fit of this model to the experimental data shows that the potential barrier is sufficiently high in the low temperature phase for the cations to perform a librational motion of relatively long duration in a given well. By contrast, in the high temperature phase, the motion is rather that of a slightly hindered rotator.

Tetramethyl ammonium manganese chloride,  $(\text{CH}_3)_4\text{MnCl}_3$  exhibits the properties of a one-dimensional anti-ferro magnet in its low temperature phase. These peculiar properties derive from the crystal structure where chains of  $\text{MnCl}_3$  units lie along the *c*-axis and are *insulated* from one another by parallel chains of tetramethylammonium ions.

Apart from its peculiar magnetic properties,  $\text{N}(\text{CH}_3)_4\text{MnCl}_3$  is remarkable in the orientational motion of its polyatomic cations. This gives rise to an orientational phase transition at 128 K. In the high temperature phase ( $P 6_3/m$ ,  $Z = 2$ ) the cations are

very probably orientationally disordered along the hexad axis [1]. The low temperature crystal [2] derives from the high temperature one by doubling of one of the lattice constants in the hexagonal plane ( $Z = 4$ ) with little changes in other cell parameters. The space group becomes  $P 2_1/a$ , with  $\beta = 120.69^\circ$  as a remnant of the hexagonal structure. The doubling of the unit cell allows orientational ordering of the cations to set in. Large amplitude rotational motions of the cations are predictable, taking only the form of rare rotational jumps between undistinguishable orientations in the ordered phase, whereas in the high temperature phase the motion might be less simple.

We present here a neutron scattering study which has been undertaken to get some information on this motion.

(\*) Present address : Laboratoire de Physique de la Matière Condensée (associé au C. N. R. S.), Faculté des Sciences. 06034 Nice, France.

1. **Experimental.** — The neutron spectra were observed with the 6 H neutron time of flight spectrometer on the DIDO reactor AERE Harwell [3]. The neutron's incident time of flight was 1 208.4  $\mu\text{s}/\text{m}$ . The experimental apparatus width was measured from the vanadium peak as 70  $\mu\text{s}/\text{m}$  (FWMH). Samples of  $(\text{CH}_3)_4\text{N}^+\text{MnCl}_3^-$  from Dr. M. T. Hutchings (AERE) were prepared by published methods [4] and stored in a desiccator before use. Figure 1 contrasts the time of flight spectra, for the low and high temperature phases respectively, at two angles of scattering  $\varphi = 45^\circ$  and  $\varphi = 81^\circ$  to the incident beam direction. The striking difference between the two temperatures is the transformation of the strong band at the energy transfer 32  $\text{cm}^{-1}$ , observed at 122 K, into a smooth shoulder of the quasi-elastic peak at room temperature. The same effect can be seen in data taken at 140 K which suggests that the major effect accompanies the phase transition at 128 K. We suggest that this transformation of the spectrum is due to a drastic change in the potential barrier hindering the rotational motion of the cations.

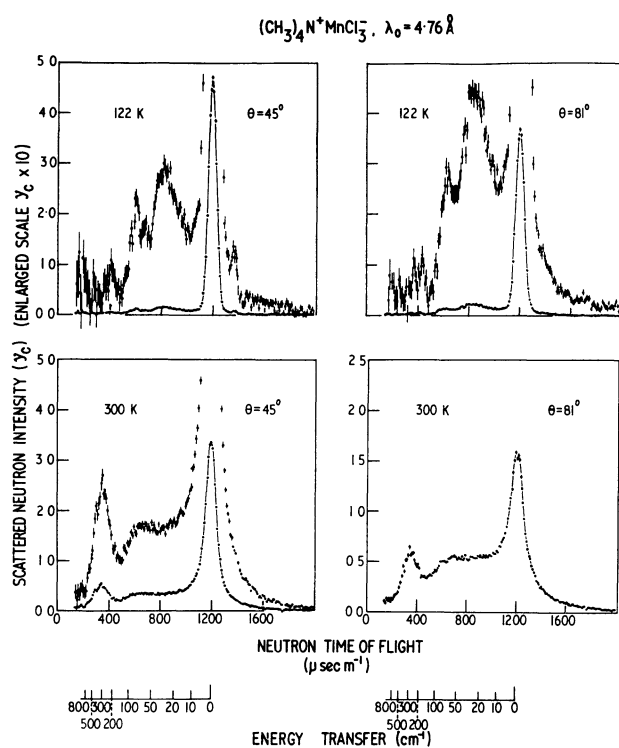


FIG. 1. — Experimental values of the neutron inelastic cross section in function of time of flight. Intensity  $\partial^2\sigma/\partial\Omega\partial\tau$  is in arbitrary unit, time of flight in micro-second/meter. a) 122 K, scattering angle :  $\theta = 45^\circ$ ; b) 122 K,  $\theta = 81^\circ$ ; c) 300 K,  $\theta = 45^\circ$ ; d) 300 K,  $\theta = 81^\circ$ .

Before proceeding to this question we remark that the positions of the peaks in the spectrum above 300  $\text{cm}^{-1}$  are rather insensitive to temperature changes through the transition region although their intensities at 122 K and 140 K are reduced substantially by the Boltzmann factor. Some changes in the widths of the

modes may occur but the resolution of the time of flight spectrometer prevents detailed exploration and measurements with a beryllium filter spectrometer are in progress [5].

The evidence above is consistent with the interpretation that the high frequency spectrum is due to internal modes of the cations. These modes are not strongly dispersed and their correspondingly high density of states makes a strong contribution to the incoherent scattering spectrum. Table I lists the frequencies of maximum scattering from the time of flight spectra in the molecular and lattice vibrational regions (above and below 300  $\text{cm}^{-1}$ ).

TABLE I

Comparison of the frequencies of intense features in the inelastic neutron scattering, INS spectra of  $(\text{CH}_3)_4\text{N}^+\text{MnCl}_3^-$  at 122 K and 296 K with optical data

INS 122 K ( $\text{cm}^{-1}$ )	INS 296 K ( $\text{cm}^{-1}$ )	Optical ( $\text{cm}^{-1}$ )
$32 \pm 2$		
$39 \pm 2$		
$48 \pm 5$		
$67 \pm 4$	63	
$84 \pm 4$	$78 \pm 4$	(*) 88 $E_{2g}$
$98 \pm 4$	$100 \pm 5$	
120		(*) 118 $E_{1g}$
		(*) 129 $E_{2g}$
		(*) 182 $E_{2g}$
$210 \pm 10$		
$297 \pm 10$	$280 \pm 10$	(*) 256 $A_g$
	$327 \pm 20$	(+) 369 (TM)
	$415 \pm 15$	(+) 457 (TM)

(\*) Référence [5],

(+) Référence [2].

The three relatively strong lines at 100, 88 and 74  $\text{cm}^{-1}$  respectively (122 K) have probably the same origin as the 91  $\text{cm}^{-1}$  IR and the 88  $\text{cm}^{-1}$  Raman lines, i. e. mainly translational motion of the cations [6] (the fact that the neutron and the optical frequencies are not identical can be explained by experimental error or by a slight dispersion in the corresponding branches).

2. **Qualitative interpretation.** — Considering now the region around 32  $\text{cm}^{-1}$  and the rotational motion of the cations, we first remark that this motion is likely to be very anisotropic. We notice indeed, that the tetramethyl ammonium ions are strongly distorted from their natural  $T_d$  symmetry [1]: the C-N-C angle which lies perpendicular to the hexagonal plane is 106.25°, i. e. smaller than the tetrahedral angle, whereas the C-N-C angle in this plane is greater (112.50°). This seems to indicate a state of stress of the cation in the direction of the hexad (3) axis.

Consequently, inplane reorientational motion is thought to be easier, i. e. reorientation about the  $C_3$  axis of the cation site. Adopting this hypothesis, we consider the rotational motion of the cations about the corresponding directions in both phases (hexagonal direction at HT, monoclinic direction at LT). Each cation sees, for this motion, a potential of  $C_3$  symmetry (in the LT phase, this is only approximate, but reasonable since the distortion of the hexagonal to monoclinic lattice is very small (see introduction)). We adopt, «*faute de mieux*», the usual sinusoidal potential :

$$V = \frac{1}{2} V_0(1 - \cos 3 \theta) \quad (1)$$

If such a potential has deep enough wells ( $V_0$  large), the thermal angular motion can be analyzed into librations in a well, interrupted by rare reorientational jumps above the barrier separating the wells. This is probably the situation in the low temperature phase : the peak at  $32 \text{ cm}^{-1}$  can be interpreted as arising from this librational motion. Applying the harmonic approximation since the wells are deep, we obtain for the librational frequency the value :

$$\bar{\nu} = \frac{3}{2} \pi c \left( \frac{V_0}{2I} \right)^{1/2} \quad (2)$$

where  $I$  is the moment of inertia ( $160.10^{-40} \text{ g.cm}^2$ ). With  $\bar{\nu} = 32 \text{ cm}^{-1}$  at 122 K this yields :

$$V_0 \approx 8 \text{ kJ/mole} \approx 2 \text{ kcal/mole} .$$

With such a high barrier ( $7.5 kT$  at 122 K) the orientational jumps from one well to another are such rare events that the long time decay of the correlation function (CFs) of the spherical harmonics bound to the ions is very slow, so that the corresponding broadening of the quasi-elastic peak is not detectable.

In the high temperature phase the spectra immediately show that the situation is very different : the shouldered shape of the spectrum in the  $20\text{-}40 \text{ cm}^{-1}$  region indicates a trend toward much more free rotation. This lowering of the barrier at the transition can be explained even if the specific volume increment is small : the change in repulsive energy  $dE/dR$  ( $R$  being an intermolecular distance) is due to the peripheral atoms of the pluriatomic reorienting species. If, as in the present case,  $R$  is large,  $R dE/dR$  is large also, so that a small *relative* expansion can lower considerably the barrier.

**3. Numerical model for hindered rotation.** — Tentatively, we adopt the following model, which is analogous to models previously proposed for potentials of different symmetries [7], [8].

A plane rotator with a moment of inertia  $I$  lies in the potential (1). Its contact with the surrounding thermal bath is simulated by torque impulses occurring at random times governed by a Poisson distribution with a characteristic time  $\tau_i$ . At each impulse a new angular velocity  $\dot{\theta}$  is randomly chosen in accord with the

Boltzmann distribution  $f(\dot{\theta})$  pertinent for the given temperature :

$$f(\dot{\theta}) = \left( \frac{I}{2 \pi kT} \right)^{1/2} \exp \left( - \frac{I \dot{\theta}^2}{2 kT} \right).$$

The natural motion of the rotator in the potential is integrated between the impulses. The desired time correlation functions are extracted by numerical averaging of a long computational run comprising at least a few hundred impulses.

This model, in which the CFs have the correct inertial second derivative at  $t = 0$ , has the advantage that a whole range of hindering can be treated, from deep orientational trapping to free rotation with self inclusion of the anharmonicity in the intermediate cases. In common with many other models, its drawback lies in the adoption of instantaneous collisions (torque impulses) to simulate the interactions with the thermal bath, i. e. the interaction of the rotational motion of the molecule with the phonons. For deep wells the model yields damped librational motion in the wells plus rare changes of wells (when a torque impulse happens to yield sufficient rotational kinetic energy). For shallow potentials the motion is a perturbed non uniform rotation.

The application of the model to neutron scattering is facilitated by the utilization of the Sears' formalism [9], i. e. expansion of the rotational part of the scattering function in terms of Fourier Transforms of the time correlation functions of the successive spherical harmonics

$$S_{\text{rot}}^{\text{inc}}(\mathbf{Q}, \omega) = \sum_{l=0}^{\infty} (2l+1) J_l^2(Qd) \tilde{F}_l(\omega) \quad (3)$$

where

$$\tilde{F}_l(\omega) = \frac{1}{2\pi} \int_{-\infty}^{+\infty} dt e^{-i\omega t} F_l(t), \quad (4)$$

$J_l$  is a spherical Bessel function,  $d$  is the distance between the proton and the center or axis of rotation, and  $F_l(t)$  is the time correlation function for the spherical harmonic of order  $l$  : this can be written :

$$F_l(t) = (2l+1) \langle P_l(\cos \theta(0)) P_l(\cos \theta(t)) \rangle \quad (5)$$

where  $\theta$  is the angle of  $\mathbf{d}$  with an arbitrary laboratory fixed axis, and  $P_l$  is the Legendre polynomial of order  $l$ .

For an isotropic medium, even a polycrystal, an isotropic average of the direction of this axis with respect to the initial direction of  $\mathbf{d}$  must be made. Formula (5) then reduces to :

$$F_l(t) = P_l \langle \cos \Theta(t) \rangle, \quad (5')$$

where  $\Theta$  is the angle between the orientation of  $\mathbf{d}$  at time 0 and its orientation at time  $t$  later (<sup>1</sup>). One has  $F_l(0) \equiv 1$ ,  $F_0(t) \equiv 1$ .

(<sup>1</sup>) See appendix.

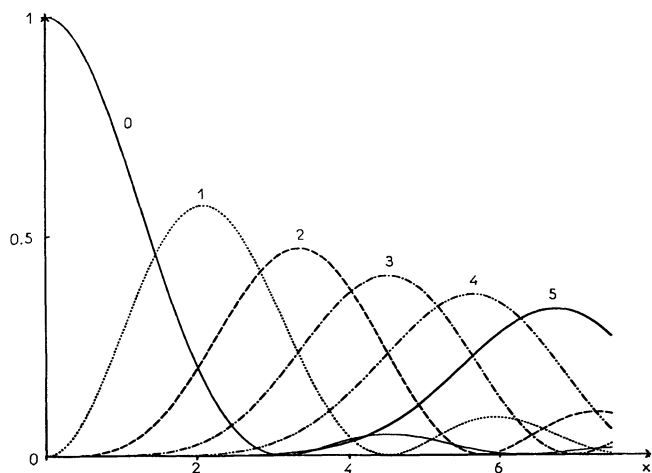


FIG. 2. — Numerical values of  $(2l+1)J_l^2(x)$ . —  $l = 0 \dots l = 1$   
 - - -  $l = 2$  — — —  $l = 3$ ; - . . -  $l = 4$  —  $l = 5$ .

It has been suggested [10] that, for not too large wave vector transfers  $Q$ , it is sufficient to limit the

above series to  $l = 1$  (Gaussian approximation). We will first check the range of validity of this approximation: Figure 2 shows, for different  $l$ , the values of  $(2l+1)J_l^2(Qd)$  versus  $Qd$ . It is seen that in the case of the  $N(CH_3)_4^+$  ion, where  $d$  is not very small ( $\sim 2.0 \text{ \AA}$ ), the second and higher order terms become important as soon as  $Q$  reaches say  $1 \text{ \AA}^{-1}$ . This is the case in the  $800 \mu\text{s/m}$  region of our experimental spectra: one has there, at the scattering angle  $54^\circ$ ,  $Q = 1.6 \text{ \AA}^{-1}$ , i. e.  $Qd = 3.2$ . Consequently we have computed the CFs up to  $l = 5$ , in order to be conservative.

In a liquid all successive CFs go to zero at infinite times. The situation is however different in crystals, because there exist privileged orientations separated by definite angles. The infinite-time value of each CF is an equilibrium property which is easy to calculate:

With the potential described by eq. (1), all orientations are coplanar, and letting

$$\Theta(\infty) = \theta(\infty) - \theta(0) \equiv \theta_1 - \theta_0,$$

one has:

$$F_l(\infty) = \frac{\int_0^{2\pi} d\theta_0 \exp -\frac{V(\theta_0)}{kT} \int_0^{2\pi} d\theta_1 P_l \cos(\theta_1 - \theta_0) \exp -\frac{V(\theta_1)}{kT}}{\left[ \int_0^{2\pi} d\theta \exp -\frac{V(\theta)}{kT} \right]^2}. \quad (6)$$

3.1 DEEP WELLS CASE (LOW TEMPERATURE). — For large  $V$  the librational motion and the rare orientational jumps from one well to another one are well separated. The second phenomenon gives rise to a slow exponential decay of the CFs at long time toward their respective asymptotical values.

First, as an illustration, we give the theoretical results for very large  $V$ : neglecting the small amplitude librational motion in the then very narrow wells (at fixed  $kT$ ), the motion can be considered as jumps between three discrete orientational sites. Calling  $k_0$  the common probability of jump towards a given neighbouring site <sup>(2)</sup>, and taking the rotator initially in site (1) (this is allowed since all three sites are equivalent), one has for the probability of presence in each well at time  $t$ :

$$\begin{aligned} N_{(1)}(t) &= \frac{1}{3} + \frac{2}{3} \exp(-3 k_0 t) \\ N_{(2)}(t) &= N_{(3)}(t) = \frac{1}{3} - \frac{1}{3} \exp(-3 k_0 t). \end{aligned} \quad (7)$$

Hence:

$$\begin{aligned} F_l(t) &= N_{(1)}(t) + N_{(2)}(t) P_l \left( \cos \frac{2\pi}{3} \right) + \\ &\quad + N_{(3)}(t) P_l \left( \cos \frac{4\pi}{3} \right). \end{aligned}$$

(2)  $k_0$  can be calculated using equipartition [11]. We will not need its value.

Or:

$$\begin{aligned} F_1(t) &= \exp(-3 k_0 t) \\ F_2(t) &= \frac{1}{4} + \frac{3}{4} \exp(-3 k_0 t) \\ F_3(t) &= \frac{5}{8} + \frac{3}{8} \exp(-3 k_0 t) \\ F_4(t) &= \frac{9}{64} + \frac{55}{64} \exp(-3 k_0 t) \\ F_5(t) &= \frac{35}{128} + \frac{93}{128} \exp(-3 k_0 t). \end{aligned} \quad (8)$$

(The constant terms in this expression could have been obtained by replacing the integrals in (6) by sums over three discrete values of  $\theta_0$  and  $\theta_1$ .)

Passing now to the fit of the model of tetramethylammonium manganese chloride at 122 K, we adopt  $V = 7.5 kT$  as said above. Our choice of  $\tau_i$ , guided by the width of the experimental peak at  $32 \text{ cm}^{-1}$ , is  $0.8(I/kT)^{1/2} = 0.8 \times 10^{-12} \text{ s}$ . The results for the numerically computed CFs are shown on figure 3. It is seen that the librational oscillations are clearly visible, but that the long time decay is excessively slow ( $k_0$  very small). The theoretical values (6) towards which the function would tend at very long time are  $F_1(\infty) = 0$ ,  $F_2(\infty) = 0.250$ ,  $F_3(\infty) = 0.455$ ,  $F_4(\infty) = 0.1406$ ,  $F_5(\infty) = 0.1990$ .

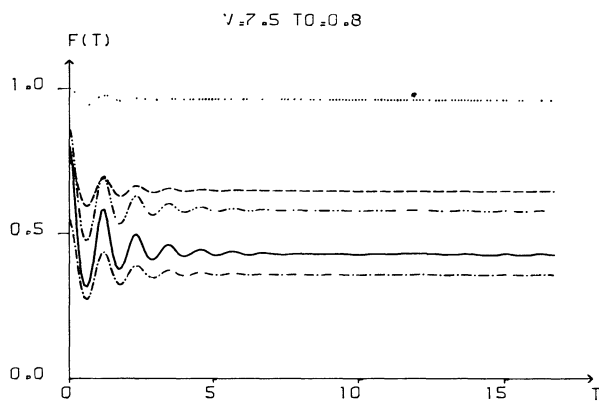


FIG. 3. — Model correlation functions  $F_l(t)$ ,  $l = 1$  to  $5$ ;  $V = 7.5 kT$ ,  $\tau_1 = 0.8 \sqrt{l/kT}$  (low temperature) (linear scale of the ordinates). Same convention for  $l$  as in figure 2.

In fact since these values are not reached we use instead the following values which are the values of the CFs after that the initial librational behaviour has decayed :

$$y_1 = 0.968, \quad y_2 = 0.655, \quad y_3 = 0.36, \\ y_4 = 0.59, \quad y_5 = 0.434. \quad (9)$$

These initial oscillatory parts of the CFs have been numerically Fourier transformed for use in eq. (3) while the weight of the elastic part is given by :

$$\sum_l (2l + 1) J_l^2(Q, d) y_l. \quad (10)$$

3.1.1 *Elastic Form Factor.* — The computed values of eq. (10) have been plotted in semi-log form in figures 4a 122 K, 4b 300 K. The calculated scattering cross section accounts for only one rotational degree of freedom and in the low temperature phase the inelastic and elastic components are well separated. This

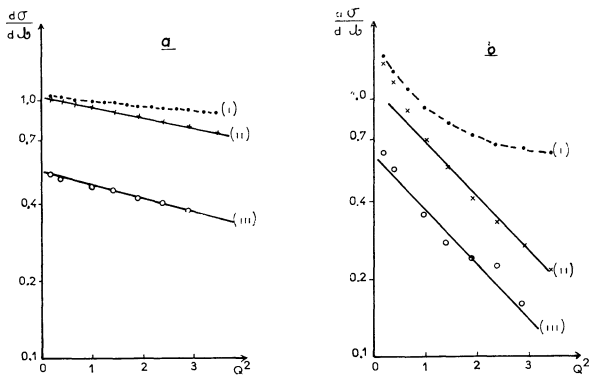


FIG. 4. — Intensity of the elastic peak maximum as function of (momentum transfer)<sup>2</sup>,  $Q^2$ , ( $\text{\AA}^{-2}$ ) at a) 122 K, b) 300 K : (i) rotational model. (ii) rotational model multiplied by  $\exp(-aQ^2)$ . (iii) experimental points.

is not so in the high temperature phase and so the expected linear dependence of log elastic intensity on  $Q^2$  is modified (Fig. 4b (i)).

If the curve had been a straight line, it could be termed a *rotational Debye-Waller factor*. The curves (iii) in figure 4 show the experimental dependence of log (elastic intensity) on  $Q^2$  and contain contributions to the Debye-Waller factor from all translations and rotations, sufficient even at 300 K to submerge the deviations noted above for the one dimensional rotational part.

The form of the elastic cross section is

$$\left(\frac{\partial\sigma}{\partial\Omega}\right)_{\omega=0} \propto \exp(-\alpha Q^2) \quad (11)$$

with  $\alpha = 0.1 \text{\AA}^2$  at 122 K.

To account for the translational and two further rotational degrees of freedom we have multiplied the rotational contribution (computed values of eq. (10)) by  $\exp(-aQ^2)$  at each  $Q$ . The quantity  $a$  is an empirical factor with values  $0.03 \text{\AA}^2$  (at 122 K) and  $0.3 \text{\AA}^2$  (at 300 K) fitted so that this product has the same slope as the experimental Debye-Waller factor (eq. (11)).

4. *Total computed spectrum.* — Finally the scattering cross section at constant angle per unit time of flight is :

$$\frac{\partial^2\sigma}{\partial\Omega \partial\tau} \sim \frac{|\mathbf{k}_1|}{|\mathbf{k}_0|} \cdot \left(\frac{m}{\tau^3}\right) \exp\left(-\frac{E}{kT}\right) \times \\ \times \{ S_{\text{rot}}^{\text{inc}}(\mathbf{Q}, \omega) * \text{RF} \} \exp(-aQ^2) \quad (12)$$

$\mathbf{k}_0, \mathbf{k}_1$  : incident and scattered neutron's wave vector.  
 $\tau$  : neutron's time of flight.

$E = E_0 - E_1$  difference between the energy of the incident and scattered neutrons.

$a$  : empirical Debye-Waller factor.

RF : spectrometer resolution function.

\* : convolution product.

$S_{\text{rot}}^{\text{inc}}(\mathbf{Q}, \omega)$  : computed rotational contribution, including elastic part (10).

The first exponential is the usual correction for the principal of detailed balance.

Eq. (12) gives a time of flight spectrum suitable for direct comparison with the experimental data although some approximations have been made for simplicity. The resolution function of the spectrometer was assumed to be gaussian in  $\omega$ . Experiments [12] show that the width of the gaussian varies by less than 10 % up to  $40 \text{ cm}^{-1}$ . Secondly, no correction to the calculated spectrum has been made for the underlying low frequency part of the translational spectrum because a reliable estimate was not available.

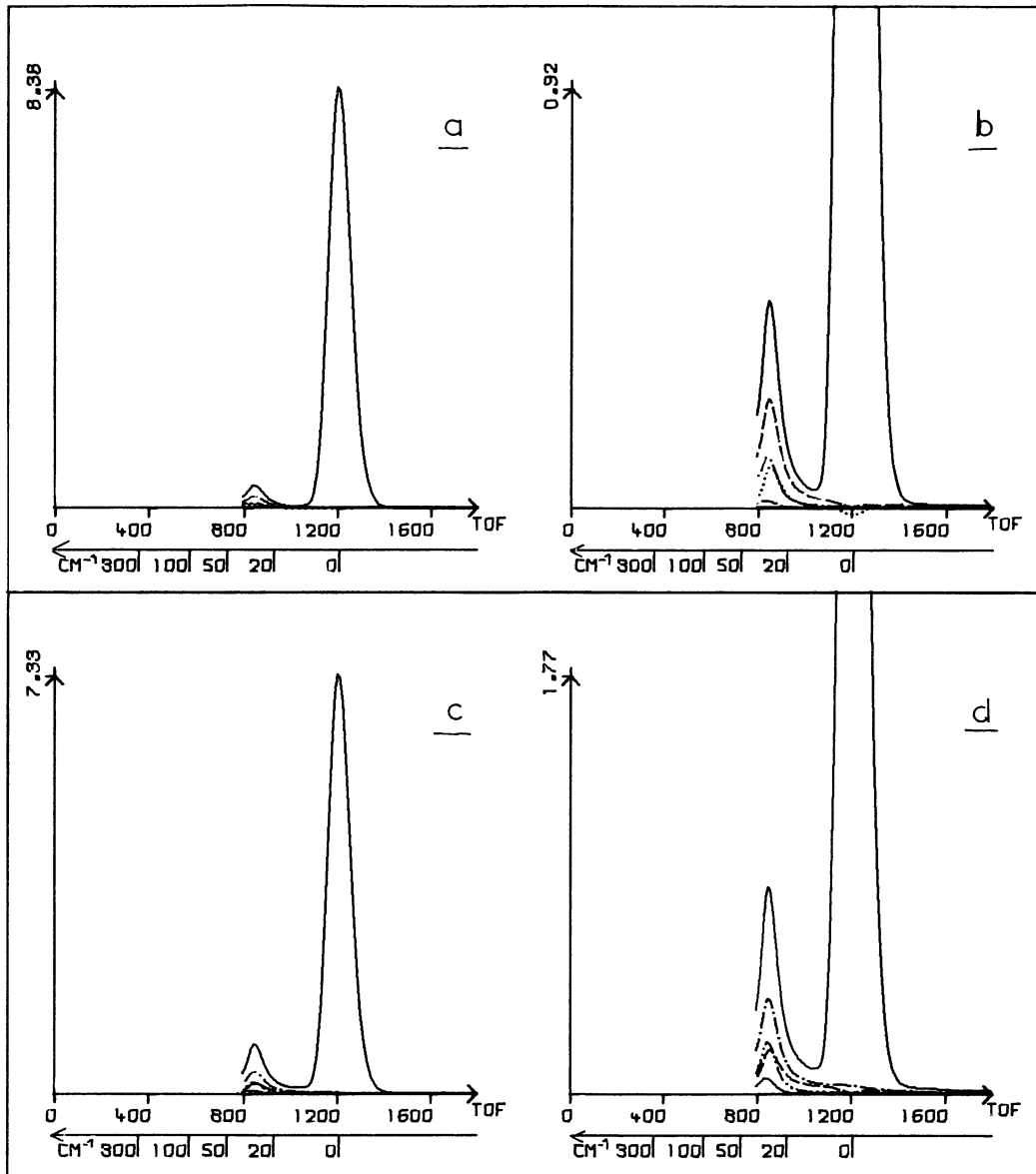


FIG. 5. — Rotational part of the scattering cross section  $(\partial^2\sigma/\partial\Omega\partial\tau)_\theta$  calculated from the model for  $V = 7.5 kT$ ,  $\tau_i = 0.5 \sqrt{I/kT}$ , a)  $\theta = 45^\circ$  and c)  $\theta = 81^\circ$ ; b) and d) expanded scale. Full line is the sum of all the contributions. The contribution of  $l = 0$  is not reported, for  $l = 1$  to 4 the partial contributions are drawn with the same convention for  $l$  as in figure 2.

Possibly the most important data needed to correct the 122 K predictions is a knowledge of the librational density of states. Our model assumes independent librational motion of the cations, hence flat librational dispersion curves and a delta function density of states whose frequency is  $32 \text{ cm}^{-1}$ . In fact at 122 K the width of the density of libration states function,  $\mathcal{L}(\omega)$ , may be greater than that of either the resolution function or any of the  $F_l(\omega)$ , so a further convolution is in principal necessary. Above the transition temperature the widths of the  $F_l(\omega)$  dominate the spectrum and the  $\mathcal{L}(\omega)$  convolution is probably unnecessary.

The time of flight spectra computed from eq. (12)

are shown in figure 5 and allowing for the approximations above the agreement with experiment, figure 1, is qualitatively good.

4.1 SHALLOW POTENTIAL CASE (297 K). — Here we have fitted the model using the parameters

$$V = 2.5 \text{ kJ/mole (i. e. } 1 kT)$$

and

$$\tau_i = 0.5 \left( \frac{I}{kT} \right)^{1/2} = 0.3 \times 10^{-12} \text{ s.}$$

We note that

$$\frac{\tau_{i300}}{\tau_{i122}} \approx \frac{0.3 \times 10^{-12} \text{ s}}{0.8 \times 10^{-12} \text{ s}} \approx 0.4.$$

This ratio is consistent with the fact that the collisions are induced by the phonons, whose density is proportional to the temperature since their population has reached its classical value in this frequency region.

To test the final exponential decay of the CF, the values of  $F_i(t) - F_i(\infty)$  have been plotted on a semi-logarithmic scale (Fig. 6), using the following values of  $F_i(\infty)$  (eq. (6)):

$$F_1(\infty) = 0, \quad F_2(\infty) = 0.250, \quad F_3(\infty) = 0.0367, \\ F_4(\infty) = 0.1406, \quad F_5(\infty) = 0.0160.$$

All correlation functions have about the same long time slope, as in the ideal case of eq. (8), which proves that the exponential decay is still due to the barrier (and not by a collision limited rotational diffusion). Initially, the CFs exhibit a few oscillations due to much anharmonic and perturbed librational motion in the shallow wells.

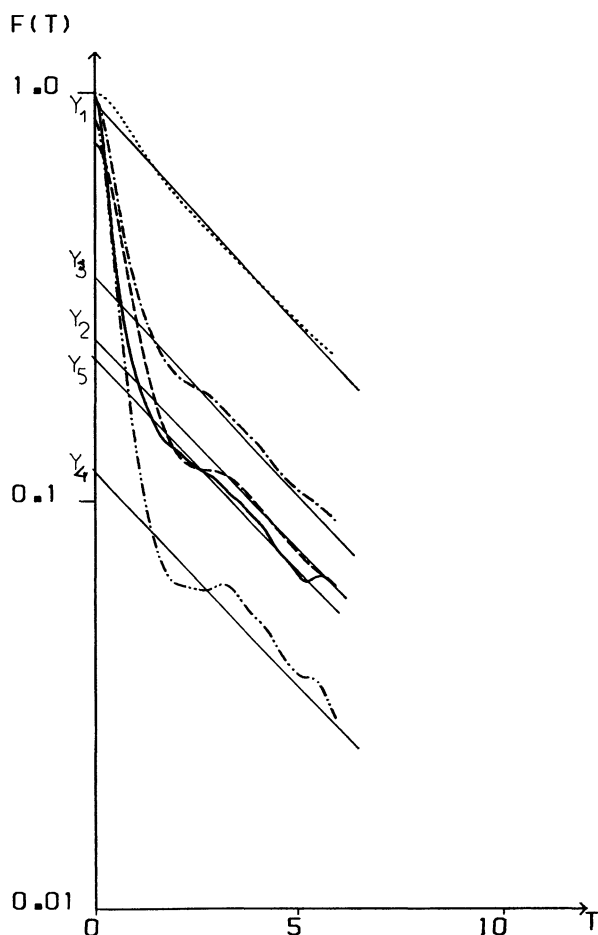


FIG. 6. — Theoretical correlation function  $F_i(t)$   $l = 1$  to  $5$ ,  $V = 1.0 kT$ ,  $\tau_i = 0.5 \sqrt{I/kT}$  (logarithmic scale for  $F(t)$ ). Same convention for  $l$  as in figure 2.

The difference between the actual values of the CFs and the value of their asymptotic exponential has been numerically Fourier transformed, while the exponential contribution has been treated analytically. The total results have been converted to time of flight spectra using the same method and same formula as explained above. The only difference is that the now discernable exponential decay of the CFs is included in the inelastic part of the spectrum while the weight of the rotational elastic part is now

$$\sum_l (2l + 1) J_l^2(Q, d) F_l(\infty).$$

This yielded the theoretical curves shown in figure 7. The computed scattering is in semi-quantitative agreement with the experimental results in the region of interest (i. e. below  $80 \text{ cm}^{-1}$ ). The flat shoulder in the  $900 \mu\text{s/m}$  region is mainly due to the short time part of the CF's (it is seen also that  $F_2$ , etc., contribute appreciably). The broadening of the quasi-elastic peak is due to the longer-time exponential decay of the CFs. The measured value of the slope of the logarithm of the maximum of the quasi-elastic peak in function of  $Q^2$  is  $\alpha = 0.435 \text{ \AA}^2$  at  $300 \text{ K}$  and with an empirical value of  $a = 0.3 \text{ \AA}^2$  we obtain an agreement with the experiments (cf. Fig. 4b).

As a final remark we note that this distinction between short and long time motions, between shoulder and quasi-elastic width has been done only for clarity. It is the more artificial the lower is the barrier hindering the motion. The numerical model employed has the advantage of yielding the CF's in the whole time scale without this artificial distinction being in principle necessary. It yields results which are qualitatively very similar to those obtained in the case of a potential of cubic symmetry [8]. In the case of the ACF of the first spherical harmonic this similarity is almost quantitative if one chooses similar values of  $V$  and  $\tau_i$ ; however with the present one-axis rotator, from the second spherical harmonic on, the ACFs do not tend to zero at long times, a situation which would appear only for higher orders in the case of cubic symmetry. This shows that if the nature of a molecular motion is to be identified with certainty, a number of different technics should be employed. Moreover, in the case of neutron scattering, with the presently available resolution and accuracy of neutron spectroscopy, it is obvious that an accurate fitting of the potential barrier of the model to the experimental data would be unwarranted, especially if the barrier is low.

We thank Dr. M. T. Hutchings, AERE, Harwell, for some preliminary results on the polarization vector of the cation rotation and for his interest in the work.

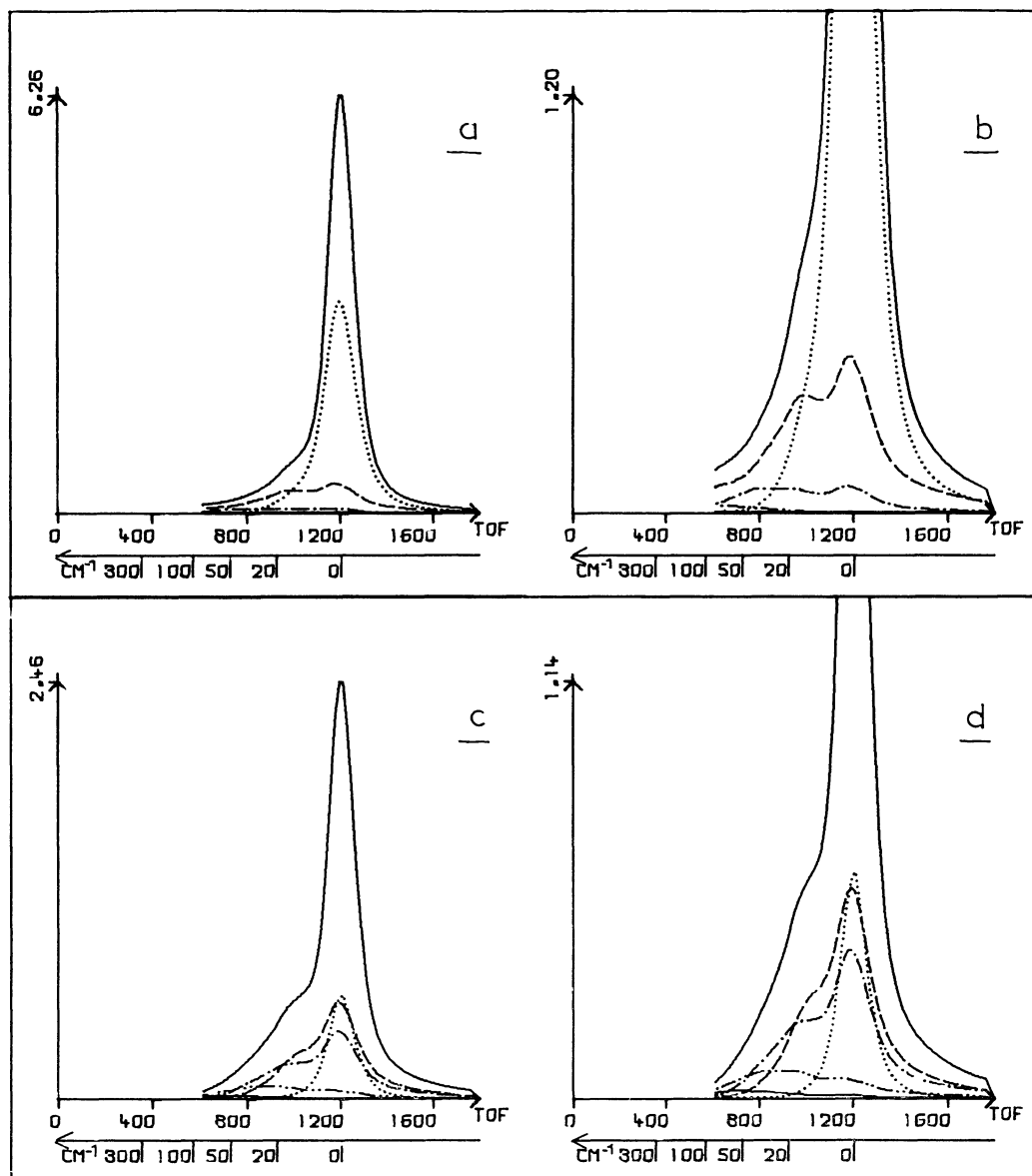


FIG. 7. — Rotational part of the scattering cross section  $(\partial^2\sigma/\partial\Omega\partial\tau)_\theta$  calculation from the model for  $V = 1.0 kT$ ,  $\tau_i = 0.5 \sqrt{I/kT}$  (high temperature), a)  $\theta = 45^\circ$ , c)  $\theta = 81^\circ$ , b) and d) dilated scale corresponding to a and c respectively. Same conventions as in figure 5.

### References

- [1] MOROSIN, B. and GRAEBER, E. J., *Acta Cryst.*, **23** (1967) 766.
- MOROSIN, B., PEERCY, P. S. and SAMARA, G. A., *Bull. Am. Phys. Soc.*, **17** (1972) 359.
- [2] PEERCY, P. S. and MOROSIN, D., *Phys. Lett.* **36A**, (1971) 409.
- [3] BUNCE, L. J., HARRIS, D. H. C. and STIRLING, G. C., Harwell Research Report, AERE, R 6246, (1970) HMSO.
- [4] HUTCHINGS, M. T., SHIRANE, G., BIRGENEAU, R. J. and HOLT, S. L., *Phys. Rev.*, **B5** (1972) 1999.
- [5] HAYWOOD, B. C., *Disc. Faraday Soc.* **48** (1969) 163.
- [6] ADAMS, D. M. and SMARDZEWSKI, R. R., *Inorg. Chem.* **10** (1971) 1127.
- [7] LASSIER, B. and BROT, C., *Disc. Far. Soc.* **48** (1969) 39.
- [8] BROT, C. and DARMON, I., *Mol. Phys.* **21** (1971) 785.
- [9] SEARS, V. F., *Can. J. Phys.* **44** (1966) 1299.
- [10] AGRAWAL, A. K. and YIP, S., *Phys. Rev.* **171** (1968) 263.
- [11] BROT, C., *Chem. Phys. Lett.* **3** (1969) 319.
- [12] REYNOLDS, P. A., KJEMS, J. K. and WHITE, J. W., *J. Chem. Phys.* **56** (1972) 2928.

**Appendix**

The aim of this appendix is to show that the Sears expansion of the intermediate scattering function in terms of average Legendre polynomials of the cosine of the reorientation angle at time  $t$  holds for a polycrystal, whatever the type or the local symmetry of the rotational motion.

Assuming (as Sears did) decoupling of the rotational from the translational motion, the incoherent intermediate scattering function factorizes into a translational and a rotational part. The latter reads :

$$I_{\text{rot}}(\mathbf{Q}, t) = \langle e^{i\mathbf{Q}\mathbf{d}(t)} e^{-i\mathbf{Q}\mathbf{d}(0)} \rangle$$

where  $\mathbf{d}$  is vector joining the center of rotation to the peripheral incoherent scatterer.

We do not use a coordinate system bound to the local crystal axis, but rather a coordinate system with  $\mathbf{Oz}$  along  $\mathbf{Q}$ . Using the well known expansion of a plane wave, we have :

$$I_{\text{rot}}(\mathbf{Q}, t) = \sum_{l=0}^{\infty} \sum_{l'=0}^{\infty} (2l+1)(2l'+1) i^l (-i)^{l'} \times \\ \times \langle P_l[\cos \theta(0)] P_{l'}[\cos \theta(t)] \rangle \cdot J_{l'}(Qd) J_l(Qd)$$

where  $\theta$  is the polar angle of the rotator, and where the angular brackets mean ensemble averaging of the local motion over initial and final orientation. The initial orientation is spherically random with respect to  $\mathbf{Oz}$ , since the crystallites are randomly oriented. Hence, at  $t = 0$ , the terms  $l \neq l'$  yield zero by orthogonality of the zonal harmonics. At finite times they yield zero also by isotropy of the motion with respect to the laboratory frame. Hence :

$$I_{\text{rot}}(\mathbf{Q}, d) = \sum_{l=0}^{\infty} (2l+1)^2 J_l^2(Q, d) \times \\ \times \langle P_l[\cos \theta(0)] P_l[\cos \theta] (t) \rangle .$$

Now a theorem on Integrals of products of surface spherical harmonics (see MacRobert, *Spherical harmonics*, Pergamon, Ch. VII, 9) yields, with a proper choice of the 3 directions involved (integral bearing on the direction of our  $\mathbf{Oz}$  with respect to  $\mathbf{d}(0)$ ) :

$$I_{\text{rot}}(\mathbf{Q}, d) = \sum_{l=0}^{\infty} (2l+1) J_l^2(Q, d) \langle P_l[\cos \Theta(t)] \rangle$$

where  $\Theta(t)$  is the angle between  $\mathbf{d}(0)$  and  $\mathbf{d}(t)$ .